

Outdoor to Indoor Penetration Loss at 28 GHz for Fixed Wireless Access

C. U. Bas¹, *Student Member, IEEE*, R. Wang¹, *Student Member, IEEE*, T. Choi¹, *Student Member, IEEE*, S. Hur³, *Member, IEEE*, K. Whang³, *Member, IEEE*, J. Park³, *Member, IEEE*, J. Zhang², *Fellow, IEEE*, A. F. Molisch¹, *Fellow, IEEE*

¹University of Southern California, Los Angeles, CA, USA,

²Samsung Research America, Richardson, TX, USA

³Samsung Electronics, Suwon, Korea

Abstract—This paper presents the results from a 28 GHz channel sounding campaign performed to investigate the effects of outdoor to indoor penetration on the wireless propagation channel characteristics for an urban microcell in a fixed wireless access scenario. The measurements are performed with a real-time channel sounder, which can measure path loss up to 169 dB, and equipped with phased array antennas that allows electrical beam steering for directionally resolved measurements in dynamic environments. Thanks to the short measurement time and the excellent phase stability of the system, we obtain both directional and omnidirectional channel power delay profiles without any delay uncertainty. For outdoor and indoor receiver locations, we compare path loss, delay spreads and angular spreads obtained for two different types of buildings.

I. INTRODUCTION

The number of connected devices and their data requirements have been increasing exponentially. Especially with the introduction of new technologies such as augmented reality, virtual reality and Ultra-HD video streaming, monthly global IP traffic is expected to reach 278 exabytes by 2021 [1]. So far this demand for broadband internet is fulfilled mostly with fiber-optical links. An approach challenging costly fiber-optical deployments is leveraging the use of Fixed Wireless Access (FWA), also known as Local Multi-point Distribution Service (LMDS).

When combined with the large bandwidth available at millimeter-wave (mm-wave) frequencies, Gbps broadband connections to multiple users can be realized via FWA [2] [3]. The prospect of utilizing the fallow spectrum at the frequencies higher than 6 GHz fueled the interest in mm-wave propagation channel measurements [4] [5] [6]. Especially, the 28 GHz band attracts a lot of interest thanks to comparatively lower hardware and implementation costs due to a relatively lower carrier frequency.

An accurate channel model is crucial for an efficient wireless system design. Outdoor to indoor penetration loss is one of the most important factors of affecting the deployment of FWA or similar systems. Especially at mm-wave frequencies, the penetration loss is shown to be higher and highly sensitive to the small changes in the material types. Furthermore, at mm-wave frequencies, the angular characteristics of the propagation channel are of the utmost importance, since these systems envisioned to be highly dependent on the beam-forming gain to overcome higher path loss at higher frequencies [7].

Most of the current literature at 28 GHz focus on outdoor to outdoor measurements. Deviating from this trend, [8] performed outdoor to indoor measurements at 28 GHz by using

a rotating horn antenna channel sounder which can provide an accurate absolute delay information. They observed a larger number of clusters, larger excess delays and larger angular spreads indoor. However, there was a limited number of indoor RX locations and a single type of building was investigated. In [9], the authors showed that the excess loss due to outdoor to indoor penetration at 28 GHz can vary from 3 dB to 60 dB depending on the RX location and the construction material types. Ref. [10] investigates the penetration loss for external and internal walls at different carrier frequencies ranging from 0.8 GHz to 28 GHz, and proposes a linear model for frequency dependency of the penetration loss. In [11], the authors present results for penetration loss and reflection coefficient measurements for different types of building materials. For example; the penetration loss for clear glass is measured as 3.9 dB while it is 40 dB for tinted glass. A summary of penetration loss results, and a frequency-dependent model, is given in [12] and also used in 3GPP. None of references [9]–[12] provide any delay or angular statistics.

There are other studies investigating the outdoor to indoor propagation channel at different mm-wave frequencies. Ref. [13] provides delay and angular statistics at 20 GHz. For a urban microcellular environment, [14] presents the penetration loss at 26 GHz and 37 GHz, and compares these with microwave frequencies. Finally the references [15], [16] and [17] discusses outdoor to indoor propagation measurement campaigns performed around 60 GHz.

In this work, we present the results from a 28 GHz channel sounding campaign performed to investigate the effects of outdoor to indoor penetration on the channel characteristics for a fixed wireless access scenario. Similar to a real deployment, the measurements capture the combined effect of path loss, foliage loss and the outdoor to indoor penetration loss. A real-time channel sounder equipped with phased array antennas was used for the measurements [18]. The phased arrays form beams at the different TX and RX angles and switch between these beams in microseconds, enabling directionally resolved results while ensuring minimal variation in the environment during the measurements. We provide examples of power delay profiles and extracted multi-path components (MPC) and compare path loss, delay spread and angular characteristics for indoor and outdoor RX locations.

The rest of the paper is organized as follows. Section II describes the measurement equipment and the configuration during this channel sounding campaign. Section III provides

Table I
SOUNDER SPECIFICATIONS

Hardware Specifications	
Center Frequency	27.85 GHz
Instantaneous Bandwidth	400 MHz
Antenna array size	8 by 2
Horizontal beam steering (RX/TX)	360° / 90°
Horizontal 3dB beam width	12°
Vertical beam steering (RX/TX)	-30° to 30° / 0
Vertical 3dB beam width	22°
Horizontal/Vertical steering steps	5° / 10°
Beam switching speed	2 μ s
TX EIRP	57 dBm
RX noise figure	\leq 5 dB
ADC/AWG resolution	10/15-bit
Data streaming speed	700 MBps
Sounding Waveform Specifications	
Waveform duration	2 μ s
Repetition per beam pair	10
Number of tones	801
Tone spacing	500 kHz
PAPR	0.4 dB
Total sweep time	101.08 ms (each 90° RX Sector)

details about the two measurement scenarios under investigation. Section IV presents results for path loss, delay and angular statistics for indoor and outdoor RX locations. Finally, Section V summarizes results and suggests future work.

II. MEASUREMENT SETUP

In this campaign, we used a switched-beam, wide-band mm-wave sounder with 400 MHz real-time bandwidth [18]. The sounding signal is a multi-tone signal which consists of equally spaced 801 tones covering 400 MHz. A low peak to average power ratio (PAPR) of 0.4 dB is achieved by manipulating the phases of individual tones as suggested in [19]. This allows us to transmit with power as close as possible to the 1 dB compression point of the power amplifiers without driving them into saturation.

Both the TX and the RX are equipped with 2 by 8 rectangular phased array antennas capable of forming beams that can be electronically steered with 5° resolution in the range of $[-45^\circ, 45^\circ]$ in azimuth and $[-30^\circ, 30^\circ]$ in elevation. During this measurement campaign we utilize a single elevation angle 0° with 19 azimuth angles for the TX, and 7 elevation angles along with 19 azimuth angles for the RX. With an averaging factor of 10, the total sweep time is 101.08 ms for 2527 total beam pairs. Since phased arrays cover 90° sectors, we rotated the RX to $\{0^\circ, 90^\circ, 180^\circ, 270^\circ\}$ to cover 360° while using a single orientation at the TX. Consequently, for each measurement location, we obtain a frequency response matrix of size 7 by 72 by 19 by 801.

Moreover, thanks to the beam-forming gain, the TX EIRP is 57 dBm, and the measurable path loss is 159 dB without considering any averaging or spreading gain. Including the averaging ratio used in this campaign the measurable path-loss is 169 dB. By using GPS-disciplined Rubidium frequency references, we were able to achieve both short-time and long-time phase stability. Combined with the short measurement



Figure 1. TX and RX locations for SFU

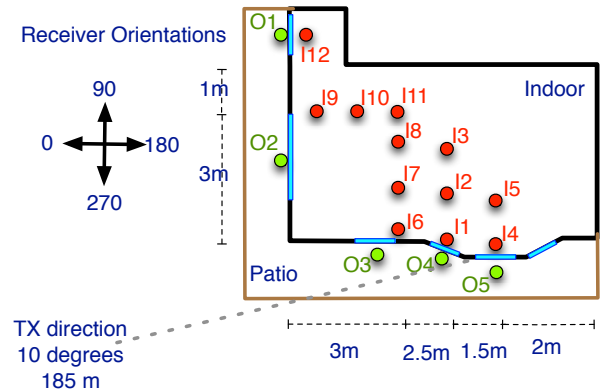


Figure 2. Layout of receivers for SFU

time this limits the phase drift between TX and RX, enabling phase-coherent sounding of all beam pairs even when TX and RX are physically separated and have no cabled connection for synchronization. Consequently, the directional power delay profiles (PDP) can be combined easily to acquire the omnidirectional PDP. Table I summarizes the detailed specification of the sounder and the sounding waveform. References [18] and [20] discuss further details of the sounder setup, the validation measurements, and the data processing.

III. MEASUREMENT CAMPAIGN

The measurements were performed at two different locations on the University of Southern California campus. In both cases, the RX was on the first floor, while the TX height was on a scissor lift at the height of 5 m imitating an urban micro-cell (UMi) scenario. To investigate the more challenging cases, we chose buildings surrounded by foliage and made sure the angle of the direct path is narrow with respect to the front facade of the target building.

A. Single Family Unit

Figure 1 shows TX and RX locations on the campus for the first location. The building is a two-story, detached, single family unit using wood frames, as is typical in California. There is also a covered, first-floor patio wrapping around the building. Measurement points are marked in Figure 2. There are 5 outdoor points placed right in front of the windows on the patio. 12 indoor measurement locations are placed throughout the room as the furniture allows. All RX points have the same height. The TX is placed on the same street with the house at a distance of 185 m at an angle of 10° according to the given

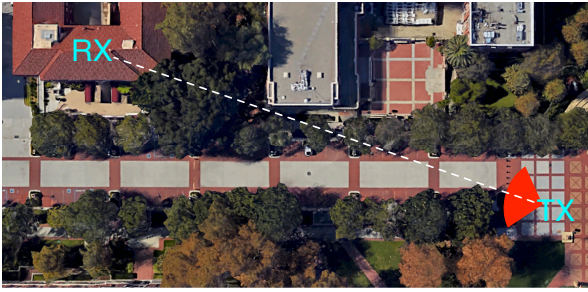


Figure 3. TX and RX locations for MSB

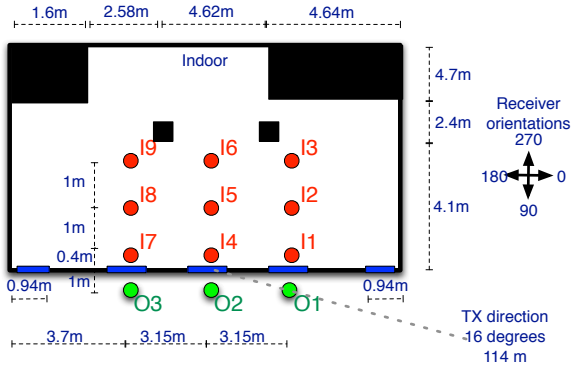


Figure 4. Layout of receivers in the MSB

directions in Figure 1. The direct path from TX to the house is blocked by foliage from trees. Additionally, points *O1* and *O2* are also shadowed by the building across the street.

B. Multi-Story Building

The second building is a multi-story, brick building (MSB) surrounded by heavy foliage as shown in Figure 3. The TX-RX distance is 114 m, and the angle of the direct path is 16° . Three outdoor measurement locations are just outside of the three front-facing windows. For each window, there are three indoor locations placed on a line along with the corresponding outdoor point. The distances from the indoor measurement points to the window are 40 cm, 1.4 m and 2.4 m, Figure 4.

IV. RESULTS

In this section we compare the path-loss, root mean square delay spreads (RMS-DS) and direction of arrival (DoA) statistics for outdoor and indoor measurements for both scenarios.

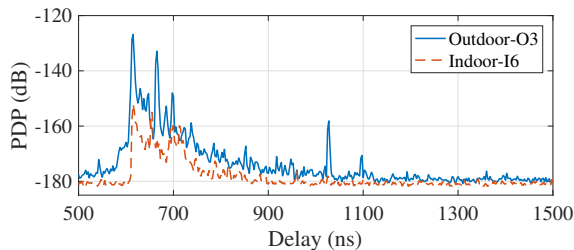


Figure 5. Power delay profiles for sample indoor and outdoor points

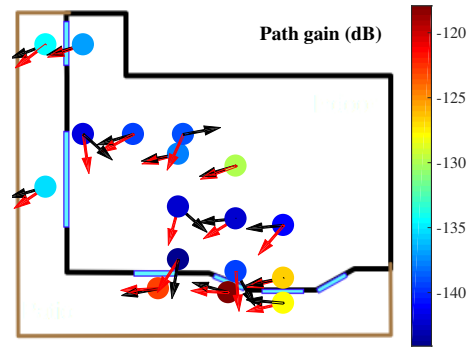


Figure 6. Path gains in dB for the RX locations in the SFU, red arrows indicate the mean direction of arrivals, black arrows indicate the RX beam direction with the highest power.

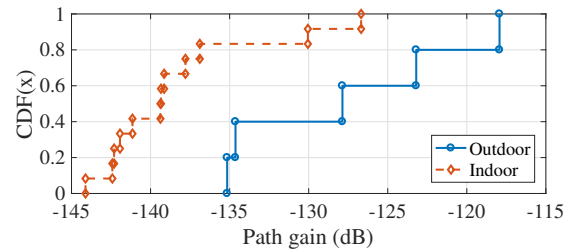


Figure 7. CDF of path gains in the SFU

A. Single Family Unit

Figure 5 shows the power delay profiles (PDP) for an outdoor (*O3*) and an indoor (*I6*) RX points. In this particular case, the excess loss due to penetration is as high as 21 dB.

Figures 6 and 7 respectively show the path gain values and their cumulative distribution functions for all RX points. The free space path loss for 185 m at 28 GHz is 106.7 dB. However due shadowing from foliage, the path-loss for the outdoor RX locations varies between 117 dB to 135 dB with a mean of 127.8 dB. According to the path-loss model in [21], based on measurements in a similar environment, the anticipated path loss is 127.4 dB for the distance of 185 m which shows a good agreement with our results. The mean path loss for indoor locations is 138.4 dB, which is 10.6 dB higher than the mean-outdoor path loss. However if the immediate points outside and inside of the windows are compared, the excess loss vary from 1 dB to 21.5 dB depending on the windows' positions.

The mean (DoA) and the directions of the RX beam with the

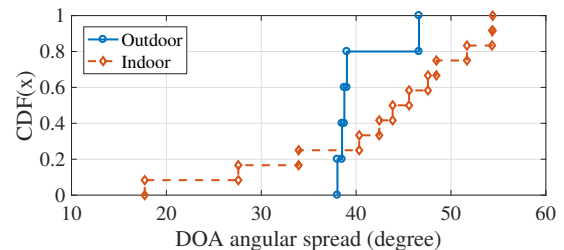


Figure 8. CDF of DoA angular spread in the SFU

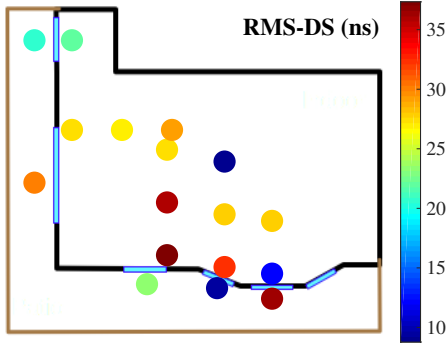


Figure 9. RMS-DS in ns for the RX locations in the SFU

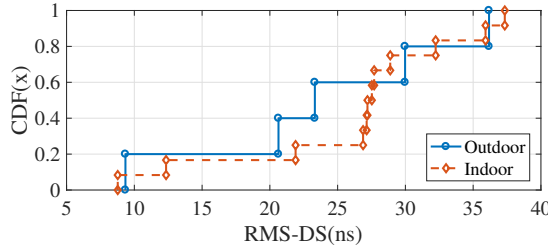


Figure 10. CDF of RMS-DS in the SFU

highest power in azimuth are also shown in Figure 6. Although the mean angular spreads are similar for outdoor and indoor measurements, the ranges of values differ significantly as seen in Figure 8. This has important implications for system design. Deployment of antennas indoors might require higher adaptivity of the antenna pattern, and the angular spread could change drastically when relocating the antenna within a room.

Figure 9 shows the RMS-DS. As also seen in the CDFs in Figure 10, indoor and outdoor RMS-DS values do not differ significantly. As summarized in Table II the means, the medians, and the ranges of RMS-DS are fairly similar for the two cases. Furthermore, when the two data sets are compared by using a two-sample Kolmogorov-Smirnov test [22], the null hypothesis of these two data coming from the same underlying distribution is not rejected with a 5% significance level.

Table II
RMS-DS (NS) FOR SFU

	Mean	Median	Max	Min
Outdoor	23.89	23.32	36.17	9.34
Indoor	26.15	27.36	37.33	8.77

B. Multi-Story Building

Figure 11 shows the path gains for all measurement locations in the MSB. Since for all indoor locations, multi-path components undergo similar propagation paths, the observed path gains don't vary significantly. The mean path losses for outdoor and indoor locations are 117 dB and 139.7 dB, respectively. Hence mean excess loss due to outdoor to indoor penetration is 22.7 dB. As anticipated, due to the brick walls and smaller number of windows compared to the SFU case, the penetration

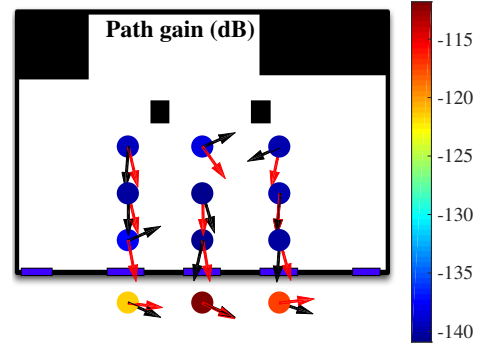


Figure 11. Path gains in dB for the RX locations in MSB, red arrows indicate mean direction of arrivals, , black arrows indicate the RX beam direction with the highest power.

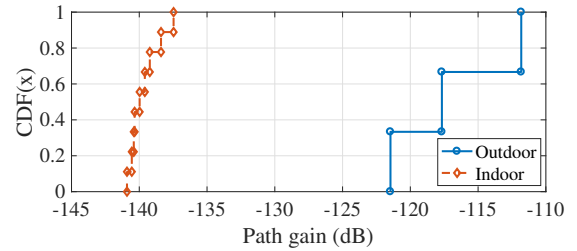


Figure 12. CDF of path gains in MSB

loss is much higher. Note that neither of these buildings uses energy-saving windows (which would have a much higher attenuation).

The detected MPCs, by using the method described in [20], are shown in Figures 14 and 15 for points *O1* and *I1*, respectively. For all indoor locations except *I6* and *I7*, we observed similar angular characteristics where all the significant MPCs are through the front windows. For those two points, the strongest MPC was the one through the hallway on the upper right side of the Figure 11. The mean angles and the direction of the best RX beams are marked with red and black arrows in Figure 11. The observed angular spreads are similar for the indoor and outdoor RX points, however, due to the limited number of outdoor locations, it is not certain that the results can be generalized. Compared to the SFU case, the observed angular spread values are within the same range. Figure 16 shows the RMS-DS. For indoor locations, we observed higher RMS-DS in MSB. In fact, the minimum RMS-DS observed

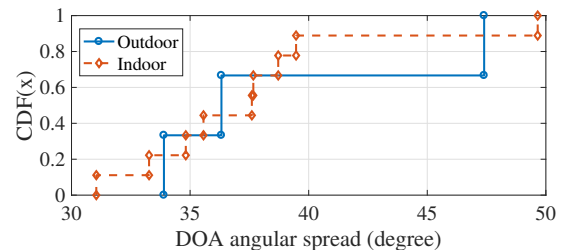


Figure 13. CDF of of DoA angular spread in MSB

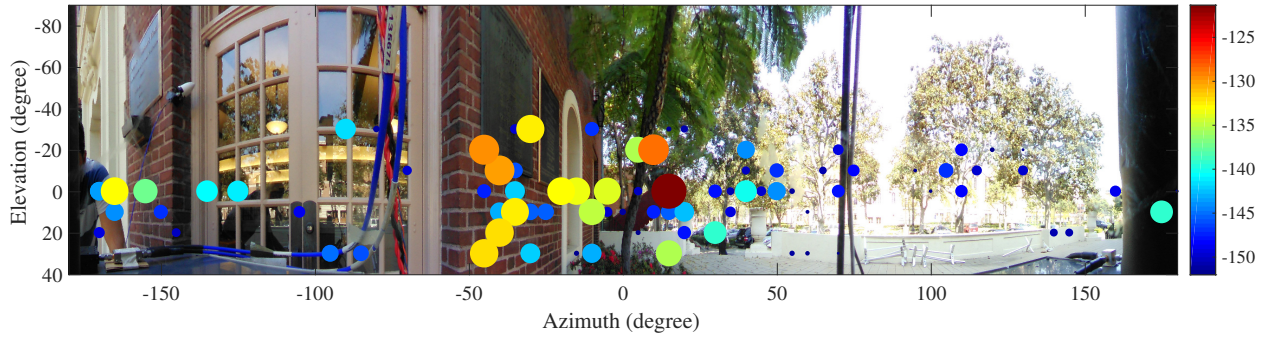


Figure 14. Detected multipath components vs DoA - outdoor *OI*

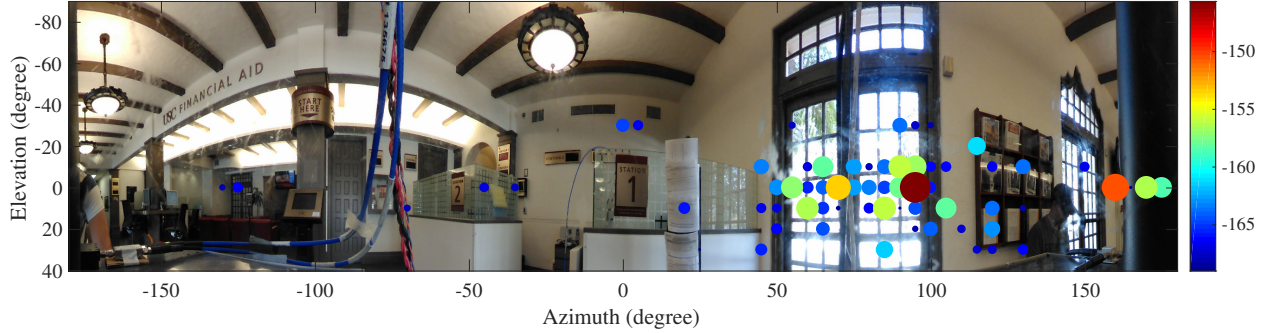


Figure 15. Detected multi-path components vs DoA - indoor *II*

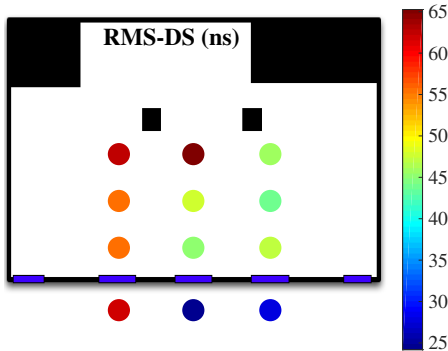


Figure 16. RMS-DS in ns for the RX locations in the MSB

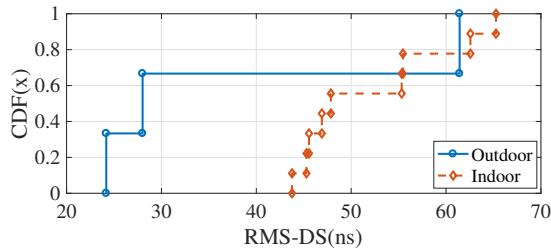


Figure 17. CDF of RMS-DS in MSB

at the MSB-indoor is larger than the maximum RMS-DS for SFU-indoor.

V. CONCLUSION

In this paper, we presented results from a channel sounding campaign focusing on outdoor to indoor wireless propagation channel for a micro-cellular scenario at 28 GHz. We presented results for path-loss, penetration loss, delay spread and angular spread statistics for two different type of housing. We observed mean excess losses of 10.6 dB for the single family unit and 22.7 dB for the multi-story brick building. For the single-family unit, we also observed that the delay spread statistics are similar for outdoor and indoor receiver locations. However, compared to the single-family unit, the delay spreads in the multi-story building were much larger. In the future, we will perform more measurements to consider other types of buildings and different receiver heights. Finally, we will also try processing the data by using high-resolution parameter extraction such as RIMAX to gain more insights.

ACKNOWLEDGEMENTS

Part of this work was supported by grants from the National Science Foundation and National Institute of Standards and Technology. The authors would like to thank Dimitris Psychoudakis, Thomas Henige, Robert Monroe for their contribution in the development of the channel sounder.

REFERENCES

- [1] C. V. Forecast, "Cisco visual networking index: Global mobile data traffic forecast update, 2016–2021 white paper," *Cisco Public Information*, 2017.
- [2] Z. Pi, J. Choi, and R. Heath, "Millimeter-wave gigabit broadband evolution toward 5g: fixed access and backhaul," *IEEE Communications Magazine*, vol. 54, no. 4, pp. 138–144, 2016.

- [3] J. Wells, "Faster than fiber: The future of multi-g/s wireless," *IEEE microwave magazine*, vol. 10, no. 3, 2009.
- [4] P. B. Papazian, G. A. Hufford, R. J. Achatz, and R. Hoffman, "Study of the local multipoint distribution service radio channel," *IEEE Transactions on Broadcasting*, vol. 43, no. 2, pp. 175–184, 1997.
- [5] A. F. Molisch, A. Karttunen, R. Wang, C. U. Bas, S. Hur, J. Park, and J. Zhang, "Millimeter-wave channels in urban environments," in *2016 10th European Conference on Antennas and Propagation (EuCAP)*, April 2016, pp. 1–5.
- [6] T. Rappaport, S. Sun, R. Mayzus, H. Zhao, Y. Azar, K. Wang, G. N. Wong, J. K. Schulz, M. Samimi, and F. Gutierrez, "Millimeter wave mobile communications for 5g cellular: It will work!" *Access, IEEE*, vol. 1, pp. 335–349, 2013.
- [7] W. Roh, J. Y. Seol, J. Park, B. Lee, J. Lee, Y. Kim, J. Cho, K. Cheun, and F. Aryanfar, "Millimeter-wave beamforming as an enabling technology for 5g cellular communications: theoretical feasibility and prototype results," *IEEE Communications Magazine*, vol. 52, no. 2, pp. 106–113, February 2014.
- [8] J. Ko, K. Lee, Y. J. Cho, S. Oh, S. Hur, N. G. Kang, J. Park, D. J. Park, and D. H. Cho, "Feasibility study and spatial-temporal characteristics analysis for 28 ghz outdoor wireless channel modelling," *IET Communications*, vol. 10, no. 17, pp. 2352–2362, 2016.
- [9] C. Larsson, F. Harrysson, B. E. Olsson, and J. E. Berg, "An outdoor-to-indoor propagation scenario at 28 ghz," in *The 8th European Conference on Antennas and Propagation (EuCAP 2014)*, April 2014, pp. 3301–3304.
- [10] I. Rodriguez, H. C. Nguyen, I. Z. Kovcs, T. B. Srensen, and P. Mogensen, "An empirical outdoor-to-indoor path loss model from below 6 ghz to cm-wave frequency bands," *IEEE Antennas and Wireless Propagation Letters*, vol. 16, pp. 1329–1332, 2017.
- [11] H. Zhao, R. Mayzus, S. Sun, M. Samimi, J. K. Schulz, Y. Azar, K. Wang, G. N. Wong, F. Gutierrez, and T. S. Rappaport, "28 ghz millimeter wave cellular communication measurements for reflection and penetration loss in and around buildings in new york city," in *2013 IEEE International Conference on Communications (ICC)*, June 2013, pp. 5163–5167.
- [12] K. Haneda, J. Zhang, L. Tan, G. Liu, Y. Zheng, H. Asplund, J. Li, Y. Wang, D. Steer, C. Li *et al.*, "5g 3gpp-like channel models for outdoor urban microcellular and macrocellular environments," in *Vehicular Technology Conference (VTC Spring), 2016 IEEE 83rd*. IEEE, 2016, pp. 1–7.
- [13] N. Tran, T. Imai, and Y. Okumura, "Outdoor-to-indoor channel characteristics at 20 ghz," in *2016 International Symposium on Antennas and Propagation (ISAP)*, Oct 2016, pp. 612–613.
- [14] T. Imai, K. Kitao, N. Tran, N. Omaki, Y. Okumura, and K. Nishimori, "Outdoor-to-indoor path loss modeling for 0.8 to 37 ghz band," in *2016 10th European Conference on Antennas and Propagation (EuCAP)*, April 2016, pp. 1–4.
- [15] M. Kim, T. Iwata, K. Umeki, K. Wangchuk, J. i. Takada, and S. Sasaki, "Mm-wave outdoor-to-indoor channel measurement in an open square smallcell scenario," in *2016 International Symposium on Antennas and Propagation (ISAP)*, Oct 2016, pp. 614–615.
- [16] L. Cheng, W. Bao, N. Liu, G. Yue, X. Zou, and R. C. Qiu, "Study of propagation characteristics of outdoor-to-indoor channel in the 60-ghz band," *Journal of Communications and Information Networks*, vol. 1, no. 2, pp. 93–101, Aug 2016. [Online]. Available: <https://doi.org/10.1007/BF03391561>
- [17] C. A. L. Diakhate, J. M. Conrat, J. C. Cousin, and A. Sibille, "Millimeter-wave outdoor-to-indoor channel measurements at 3, 10, 17 and 60 ghz," in *2017 11th European Conference on Antennas and Propagation (EUCAP)*, March 2017, pp. 1798–1802.
- [18] C. U. Bas, R. Wang, D. Psychoudakis, T. Henige, R. Monroe, J. Park, J. Zhang, and A. F. Molisch, "A Real-Time Millimeter-Wave Phased Array MIMO Channel Sounder," in *Vehicular Technology Conference, 2017. VTC 2017-Fall. IEEE*, September 2017.
- [19] M. Friese, "Multitone signals with low crest factor," *Communications, IEEE Transactions on*, vol. 45, no. 10, pp. 1338–1344, Oct 1997.
- [20] C. U. Bas and et.al., "A Real-Time Millimeter-Wave Phased Array MIMO Channel Sounder for Dynamic Measurements," to be submitted.
- [21] C. U. Bas, R. Wang, S. Sangodoyin, S. Hur, K. Whang, J. Park, J. Zhang, and A. F. Molisch, "28 GHz Microcell Measurement Campaign for Residential Environment," in *2017 IEEE Global Communications Conference (GLOBECOM)*, December 2017.
- [22] F. J. Massey Jr, "The kolmogorov-smirnov test for goodness of fit," *Journal of the American statistical Association*, vol. 46, no. 253, pp. 68–78, 1951.